Suppression of Fracture Failure at Steel/Concrete Interaction Zones by Material Ductility in ECC

Victor C. Li and Shunzhi Qian
Advanced Civil Engineering Materials Research Laboratory
Department of Civil and Environmental Engineering
University of Michigan, Ann Arbor, MI 48109-2125

Abstract

Concrete fracture failure is often observed at interaction zones between steel and concrete, including those in hybrid structure connections, shear studs in composite beams, and steel fasteners in concrete. Improvement in intrinsic ductility of the concrete material should suppress such failure mode and enhance the overall structural performance. In this paper, we introduce and experimentally demonstrate the feasibility of this concept via two case studies, i.e., the shear behavior of steel stud/ECC connection and pullout behavior of 2D anchor bolt/ECC connection. The micromechanically designed ECC (Engineered Cementitious Composite) with a tensile ductility three hundred times that of normal concrete totally eliminated the brittle fracture mode by developing extensive "plastic" deformation in both ECC and the steel stud in the first case and in ECC in the second one. This modification in behavior led to higher load capacity and ductility, thus enhancing structural response. The enhancement in structural response through material ductility engineering is expected to be applicable to a wide range of engineering structures where steel and concrete comes into contact.

Keywords: ECC, Engineered Cementitious Composite (ECC), Material ductility, Suppression of fracture failure, Steel/concrete interaction zones, Shear stud, Anchor bolt

---

Victor C. Li
The University of Michigan
2350 Hayward Street
2326 G. G. Brown
Ann Arbor, MI 48109-2125

Email:vcli@umich.edu
Tel: 734-764-3368

1.0 Introduction

1.1 Background and motivation behind proposed research

Fracture of concrete is a dominant failure mechanism when steel and concrete interact mechanically. In a wide variety of structures, such as connections involving steel studs embedded in concrete in composite beam structures, or in hybrid steel/concrete structures involving steel beams which penetrate into concrete columns, steel and concrete must interact with each other when the structure is loaded. Due to the high stiffness of steel and brittleness of concrete, failure usually occurs in the concrete in the form of fracture. A large number of RILEM round robin tests of steel anchor bolt pullout from concrete [1] demonstrate experimentally and numerically that concrete fracture is the governing failure mode and that anchor capacity is controlled by the material toughness rather than compressive strength. In the 1995 Kobe earthquake, for instance, it was observed that failure of an exposed column base (Figure 1) was due to the fracture of the surrounding concrete near the steel bolts [2]. Other examples involving concrete fracture in steel/concrete interaction zones include severe concrete spalling (Figure 2) in RC column-to-steel beam (RCS) connections due to the high bearing stress of the steel beam on concrete [3,4] and concrete cracking in the anchorage zone due to the transfer of prestressing force through steel anchorage device [5]. In the aforementioned scenarios, fracture failure of the brittle concrete at the steel/concrete interaction zones clearly compromises the safety of the structures.

Several approaches have been attempted to address steel/concrete interaction problems, with limited success. These approaches include the use of steel fiber reinforced concrete [4], steel band plates or fiber reinforced plastic wrapping [4], enlarged member section and heavy confining reinforcement [6]. While they generally result in improved behavior in steel/concrete interaction zones, the employment of these approaches is often penalized by higher cost, labor intensity, and/or space congestion. A more elegant approach is to directly impart tensile ductility into the concrete material to minimize or suppress the fracture mode of failure altogether.

A ductilized concrete material, named engineered cementitious composites (ECC) [7], offers a potential material solution to steel/concrete interaction problems. A typical tensile stress-strain curve of ECC is shown in Figure 3. As can be seen, ECC exhibits a tensile strain capacity in the range of 3-6% (300-600 times that of normal concrete or FRC) [8,9]. It attains high ductility with relatively low fiber content (2% or less of short randomly oriented fibers) via systematic tailoring of the fiber, matrix and interface properties, guided by micromechanics principles. Associated with its high ductility in tension and shear [10], ECC reveals a high damage tolerant behavior under severe stress concentration induced by steel concrete interaction in a

Figure 1: Fracture failure of concrete near steel bolt near column base of a structure during the Kobe earthquake [2]

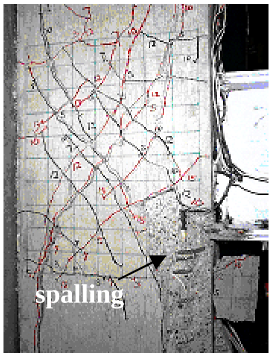

Figure 2: Fracture failure (spalling) of R/C column due to high bearing stress by steel beam [4]

number of recent experiments, such as ECC panel shear-joint test [11], RCS connection (with ECC in joint zone) test [4] and precast infill panel (made with ECC) test [12]. These tests suggest the feasibility of adopting ECC in steel/concrete interaction zone to avoid fracture failure, thus leading to significant improvements in the overall structural response.

1.2 Classes of steel/concrete interaction problems

Steel/concrete interaction problems exist in a wide variety of civil infrastructure applications. Typical steel/concrete interaction problems may be grouped into at least three broad classes associated with their structural functions: hybrid structures, fasteners and tendon/cable anchorage devices. Broadly speaking, hybrid structures include RC column and steel beam system, steel coupling beam between concrete walls, steel pile concrete cap beam system, and others. In the connection zone of these systems, steel members are embedded into the RC members. Under loads, severe bearing stress induced by steel members may cause the spalling and cracking of the adjacent concrete. The example shown in Figure 2 belongs to this class. The second broad class of steel/concrete interaction problems involves steel fasteners in concrete (sometimes also referred to as anchors in the literature), including bolts and studs, that are widely used as jointing devices in RC building and other infrastructure systems. Examples include the connection between steel girders and concrete bridge decks in transportation structures through steel shear studs, or steel bolts connecting the base plate of a steel column to a concrete base, as illustrated in Figure 1. Brittle fracture of the surrounding concrete may result from loading of the connection of the fastened members. The third class of steel/concrete interaction problems involves steel anchorage devices used to transfer prestressing forces from the steel strands into bulk concrete in prestressed concrete members. (Steel cables anchored into concrete blocks for cable stayed bridges may be regarded as other examples in this class.) Interaction between these steel components and concrete may result in brittle fracture of the concrete in the anchorage zone. Overall, it can be seen clearly that lack of ductility in concrete leads to undesirable fracture mode of failure of concrete in steel/concrete interaction zones, regardless of the actual scenarios. It is expected that this can be greatly improved by introducing ECC in the steel/concrete connection zones.

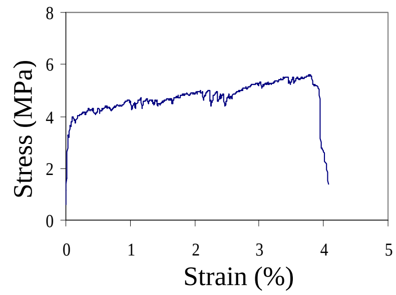

Figure 3: Typical tensile stress-strain curve of ECC

1.3 Insights from previous experimental experience

A number of recent experiments [4,11,12,13] involving the use of ECC in structural elements show significant delay or elimination of fracture localization in ECC in the interaction zones, leading to enhanced structural capacity and ductility as well as post-loading structural integrity. These experiments provide important insights into the behavior of ECC especially when compared with that of normal concrete in the high stress concentration regions induced by the interaction between steel and concrete materials.

Adoption of ECC in hybrid RCS connection combining steel beams and R/C columns results in much improved structural performance under reversed cyclic loading [4]. Despite removing all the transverse reinforcements in the connection zone, the shear strength and stiffness of the RCS connection with ECC showed a 50% increase compared with the control specimen of seismically detailed R/C connection. During earthquake, joint shear distortion performance can be used as a measure of story drift sustaining capability. The joint shear distortion of ECC RCS connection was able to increase to 0.022 rad with negligible damage while the control specimen suffered severe damage in the shear panel when joint shear distortion exceeded 0.01 rad. Of particular interest is the contrasting response of concrete and ECC at the location where the steel beam enters the R/C column. Due to the high compressive bearing stress, the concrete cover was severely spalled while the ECC showed only hairline microcracking damage (Figure 4). In addition, Parra-Montesinos and Wight [4] found that among the methods of protecting the beam-column connection (steel-band plate, hoop steel in connection, connection cover plates, steel fiber reinforced concrete, and ECC) studied, the ECC specimen showed the best damage tolerance after full reverse cyclic loading with story drifts up to 5%.

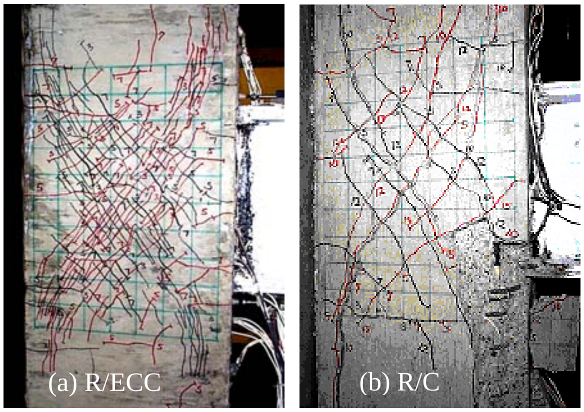

Figure 4: Comparison of RCS connections damage under reverse cyclic loading. (a) R/ECC specimen without transverse reinf. in the joint zone experienced only microcracks (<100μm) magnified by magic ink pen for clarity, and (b) R/C control specimen with standard detailing showing fracture planes with large crack width(~mm) and severe spalling.

Another example of steel/ECC interaction is afforded by a shear-joint test conducted by Kanda et al [11]. In this test, panels made with ECC and jointed together with steel bolts were loaded in shear (Figure 5). While the joints suffered microcrack damage in the ECC panels, connected fractures were revealed in the control test of similarly jointed concrete panels. The high stress induced by the steel bolts on the ECC was clearly diffused by distributed microcrack damage so that fracture localization was completely suppressed, resulting in 100% increase of the joint load capacity.

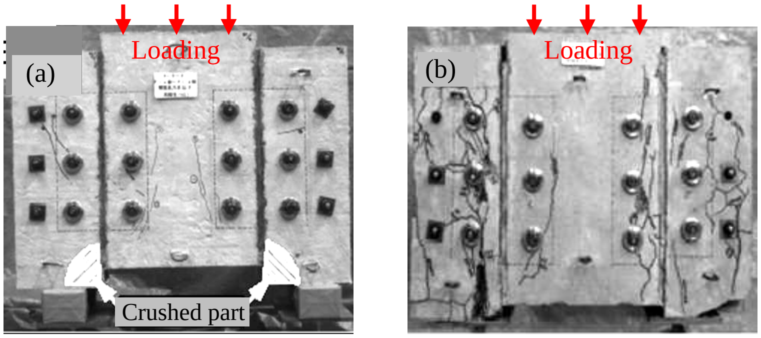

Figure 5: Shear-joint tests, showing (a) high damage tolerant behavior in ECC specimen; (b) connected fracture failure in concrete specimen

1.4 Proposed approach – material ductility to suppress concrete fracture

Observations of the influence of concrete material ductility on the structural response of the steel/concrete connections, highlighted in Section 1.3 above, strongly support the contention that material tensile ductility can be very effective in enhancing the performance of structures governed by critical connections involving steel/concrete interactions. This significant improvement in structural response is achieved by switching the failure mode from brittle fracture in concrete to ductile microcracking damage in ECC. Specifically, in the proposed study ECC will replace the concrete in steel/concrete interaction zones to investigate the feasibility of using material ductility in ECC to suppress concrete fracture failure via two case studies, i.e., the shear behavior of steel stud/ECC connection and pullout behavior of 2D anchor bolt/ECC connection.

This proposed approach exploits the ultra-ductile property of ECC, without relying on external confinement, heavy steel reinforcements and/or other measures. It is expected that this intrinsic material ductility approach is applicable to broad classes of steel/concrete interaction problems, and potentially more reliable and cost effective compared with current approaches.

2.0 Experimental Program

2.1 Materials

The concrete materials used in this study are shown in Table 1, where Concrete 1 and ECC 1 are used in steel stud/ECC connection pushout test and Concrete 2 and ECC 2 used in 2D anchor bolt/ECC connection pullout test. By uniaxial tension test, both ECC 1 and 2 show a strain capacity around 2.5% at 28 days. The moduli of elasticity of Concrete 1 and ECC 1 were measured by compression test of cylinder specimens. It is worth mentioning that the modulus measured from both compression test and uniaxial tension test of ECC specimens agree well. The shear studs used in this test were made from Grade 1018 cold drawn bars, conforming to AASHTO M169 (ASTM A108) Standard Specification for Steel Bars, Carbon, Cold-Finished, Standard Quality. The tensile strength of studs was measured to be 635 MPa.

Table 1: Mix proportion of different concrete materials by weight (fiber by volume)

Material	f_c'	E_c	ε_u	C	S	CA	FA	W	SP	Fiber
Concrete 1	52.3±3.6	28.6±1.8	0.01*	1	1.3	1.3	0	0.36	0.01	0
ECC 1	60.0±2.1	18.1±1.4	2.5	1	0.8	0	1.2	0.53	0.03	0.02
Concrete 2	45.6±1.0	-	0.01*	1	2.5	2.5	0	0.45	0.01	0
ECC 2	41.7±0.5	-	2.5	1	0.8	0	1.2	0.60	0.03	0.02

(f_c': compressive strength, unit MPa; E_c: modulus of elasticity, unit GPa; ε_u: uniaxial tensile strain capacity (%); *: assumed value; C: type I Portland cement; S: silica sands F110 for ECC1 and ECC2, ASTM C778 sand for concrete 1, 2; CA: coarse aggregate with max size 19 mm; FA: type F fly ash; W: water; SP: superplasticizer; PVA fiber: KURALON K-II REC15 (length: 12 mm, diameter: 0.04 mm, elastic modulus: 37 GPa, tensile strength: 1600 MPa), developed by Kuraray Co., LTD (Japan) in collaboration with ACE-MRL; ±: standard deviation)

2.2 Preparation of specimens and testing

The geometry of the pushout specimen is shown in Figure 6 (a). Two substrate slabs, with a dimension of 305mm x 305mm x 152 mm, were connected with a wide flange steel beam W8X40 with two shear studs welded on each side of the beam. The geometry is adopted from Ollgaard et al [14]. During casting, the material was poured from the top of the specimen. Therefore, the steel beam remained vertical to assure a horizontal loading plane. Even though this casting orientation is different from field conditions, the pouring direction is thought to be unimportant since PVA fibers in ECC are likely to be randomly distributed in a 3-dimensional state, considering the relative short fiber length with respect to the dimension of the specimen.

The concrete specimens were cured in water, and ECC specimens were cured in air to obtain favorable interface property, both for 28 days. Totally, 5 pushout specimens were tested, including 2 specimens for Concrete 1 and 3 specimens for ECC 1. Testing was conducted on a 2200 kN capacity Instron testing machine. Four LVDTs were mounted on the steel beam at the level of the shear studs to measure the slip between the beam and concrete/ECC slabs. The loading surface was ground for uniform load distribution before testing, and a ball support was used to maintain the alignment of the specimens.

Two-dimensional (2-D) anchor bolt/ECC pullout specimen is revealed in Figure 6 (b), which is adopted from the RILEM round robin test [1]. The steel anchor bolt is embedded in a thin ECC slab, with an area of 300mm by 300mm and thickness equal to 50mm. The 2D anchor bolt/ECC connection pullout test provides an opportunity for direct observation of damage evolution. In each series (concrete and ECCs) three specimens were tested. The loading was applied by an MTS 810 Material Testing System. Test was performed in displacement control mode at a rate of 0.3mm/min. The pullout displacement of the anchor bolt was measured by averaging the results of two LVDTs on both sides of the specimen. The curing conditions for ECC and concrete specimens are the same as stated above in pushout test.

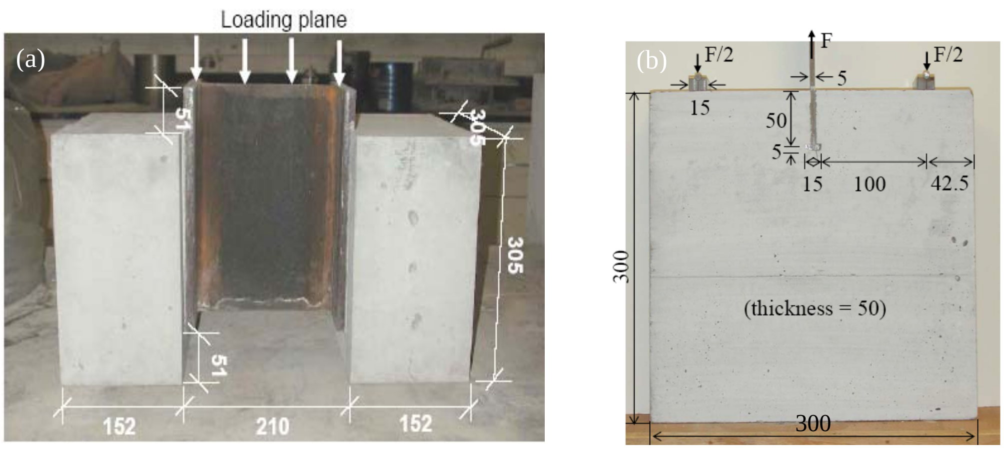

Figure 6: Geometry of (a) pushout specimen and (b) pullout specimen (unit: mm)

3.0 Results and Discussion

Overall, the proposed approach of using material ductility in ECC to suppress concrete fracture failure is successfully demonstrated and illustrated via two sets of steel/ECC interaction studies. Significant delay or elimination of fracture localization was achieved by developing extensive multiple microcracking damage in ECC instead of brittle fracture in concrete. With this drastic alteration of failure mode, the load capacity and structural ductility of steel/ECC connections were enhanced significantly. Common features of the observed failure modes and structural response for these two sets of experimental studies are briefly summarized below.

3.1 Failure mode

The failure mode of steel/ECC connections is significantly improved when compared with concrete ones due to the high tensile ductility of ECC. It switched from brittle fracture in concrete specimen to steel yielding for the pushout tests and/or multiple microcracking of ECC (in both cases) in ECC specimens.

ECC pushout specimens showed a ductile failure mode due to its extreme tensile ductility. During the initial loading stage, no cracks could be observed from the specimen surfaces. As the load increased, a few microcracks appeared, accompanied by the beginning of inelastic range in the load-slip curve. When peak load was reached, more microcracks radiated from the shear stud and developed outwards, as shown in Figure 7. In some cases, a dominant crack appeared to initiate, but rapidly diffused into many microcracks (microcrack width = 42 ± 20 μm). The final failure in the ECC specimens was associated with fracturing of the stud shank near the welds, after the stud shank underwent large plastic deformation in bending.

Conversely, in concrete pushout tests, as loading approached the peak value, large cracks (crack width about 2 mm) formed in the concrete near the shear studs and developed rapidly throughout the entire specimen as the peak load was reached. As revealed in Figure 8, concrete specimens fractured into several pieces after testing, with fracture clearly initiated from near the head of the shear studs. The high stress concentration induced by the stiff steel stud combined with the brittle nature of concrete led to the rapid development of macro cracks, resulting in the catastrophic failure of concrete pushout specimens.

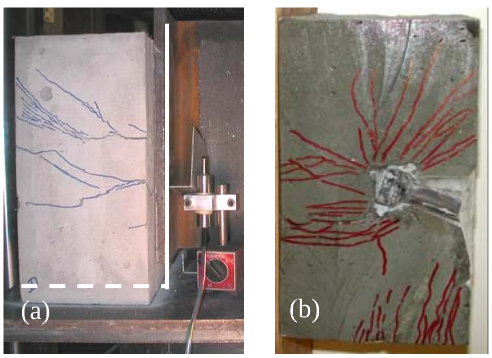

Figure 7: Half of ECC pushout specimen after test. Microcracks observed on the (a) outside and (b) inside of the half specimen (crack width ~ 40 μm, magnified by magic ink pen for clarity, cut section along shear stud indicated as white line in (a))

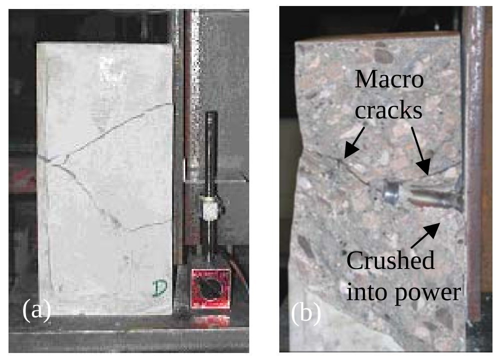

Figure 8: Half of concrete pushout specimen after test. Macro cracks observed on the (a) outside and (b) inside of the half specimen (natural fracture surface along shear stud)

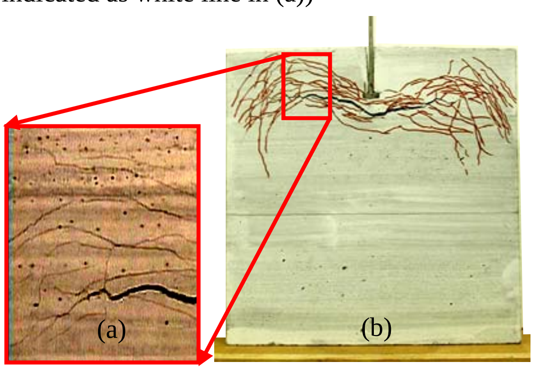

Figure 9: ECC pullout specimen after test showing ductile multiple cracking behavior in (a) close-up view (actual microcracks) and (b) overall view (microcracks magnified by magic ink pen for clarity)

Figure 10: Concrete pullout specimen after test, showing brittle fracture failure mode

Similarly, the failure mode of 2D anchor bolt/ECC pullout specimens is much more ductile than the corresponding concrete ones. As indicated in Figure 9, the microcracks (microcrack width = 57 ± 33 μm) in ECC initiated from the head of the anchor bolt and then diffused and grew in both number and length with increasing pullout load, towards the supporting points. Ultimately, as the tensile strain capacity of ECC material was exhausted, one of the microcracks localized and eventually led to the final failure of the ECC pullout specimens. It is interesting to note that the final failure crack was away from the head of the anchor bolt. In contrast, the concrete pullout specimen failed in a very brittle fracture manner (Figure 10) with fracture initiated directly from the edge of the anchor bolt head, resulting in a much lower load capacity and structural ductility in comparison to the ECC specimen. This observation demonstrated the ability of ECC to redistribute the initial highly concentrated stress near the head through a microcrack damage process.

3.2 Structural response

Closely related to its superior ductility in tension, the structural performance of the steel/ECC connection specimens was greatly enhanced compared to steel/concrete specimens in terms of load capacity and structural ductility (Figures 11 and 12), in addition to its much improved failure mode described above. It should be noted that both materials have about the same compressive strength. This suggests that material ductility in ECC plays a more significant role than compressive strength in improving the structural response of the steel/ECC connections.

Figure 11 shows the measured load per stud as a function of slip for pushout specimens. The measured strength Q_m, slip capacity S_c and crack width w_c documented in Table 2 clearly demonstrate the superior structural response of the stud/ECC connection. The ECC specimens showed on average 53% higher strength and 220% increase in slip capacity, in comparison to the concrete specimens.

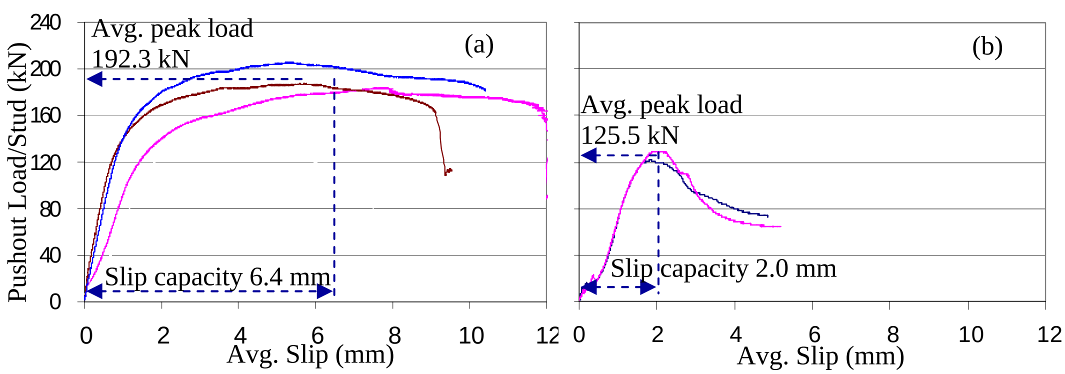

Figure 11: Measured load per stud as a function of slip for pushout specimens for (a) ECC and (b) Concrete

Table 2 Material properties and structural behavior of concrete and ECC pushout specimens

Material	ε_u (%)	f_c'(MPa)	E_c(GPa)	Q_n (kN)	Q_m (kN)	S_c(mm)	w_c(μm)
Concrete 1	0.01*	52.3±3.6	28.6±1.8	174.3±11.5	125.5±5.4	2.0±0.2	~2000
ECC 1	2.5±0.3	60.0±2.1	18.1±1.4	148.5±8.3	192.3±11.7	6.4±1.3	42±20

(ε_u: uniaxial tensile strain capacity; * assumed value; f_c': compressive strength; E_c: modulus of elasticity; Q_n: computed strength per stud; Q_m: measured strength per stud; S_c: slip capacity; w_c: crack width; ±: standard deviation)

In Table 2, Q_n is calculated from AASHTO design Eqn (1) for shear strength of a stud in concrete [15] (developed based on the test results of Ollgaard et al [14]). For both ECC and concrete specimens, the computed Q_n is governed by Eqn 1(a), which is lower than $A_{sc}F_u$ (180 kN).

$$Q_n = \min \begin{cases} 0.5 A_{sc}\sqrt{f_c' E_c} & \text{(a)} \\ A_{sc} F_u & \text{(b)} \end{cases} \qquad (1)$$

with: A_{SC} = Cross sectional area of a stud shear connector (mm^2);
= 285 mm^2 in the present experiment;
f_c' = Specified 28-day compressive strength of concrete (MPa);
E_c = Elastic modulus of concrete (MPa);
F_u = Tensile strength of a stud shear connector (MPa).

Revealed in the Table 2, the measured strength Q_m of the stud/ECC connection is about 192.3 kN, approximately 30% higher than the calculated values Q_n. This is mainly due to the fact that the compressive strength, a main contributing factor in the AASHTO design equation for studs in concrete, is not necessarily relevant to the design of stud/ECC connection, due to the switching of the failure mode. Direct adoption of the AASHTO design equation will be excessively conservative. A revised predictive equation governing strength of stud connection accounting for material ductility needs to be developed. The actual failure mechanism of ECC specimens, i.e., fracturing of stud shank near the welds, suggests that $A_{sc}F_u$ may be used in order to better predict the load capacity. Furthermore, the greatly enhanced structural ductility of stud/ECC connection needs to be addressed in the design procedure if ECC were to be used in composite structures, e.g., in the form of higher strength reduction factor. The AASHTO design equation was developed based on pushout tests of concrete with compressive strength up to 35 MPa [14], substantially lower than the concrete material used in the present test (52 MPa). Therefore, the lower measured strength Q_m compared with computed strength Q_n for Concrete 1 maybe due to potentially higher brittleness with increased compressive strength.

Similarly, the results from the anchor bolt/ECC connection pullout test show greatly enhanced structural response compared to anchor bolt/concrete connection pullout test (Figure 12). The average pullout load capacity and displacement (structural ductility) of anchor bolt/ECC connection are 20.5 kN and 1.1 mm, respectively, about twice and 16 times respectively those of concrete specimens. It should be noted that both ECC and concrete have about the same compressive strength (Table 1). Again, this reveals that compressive strength, as a traditional measurement of concrete material quality, is not necessary relevant to the structural capacity when it comes to critical steel/concrete connections since it is the fracture failure of concrete that governs the structural capacity.

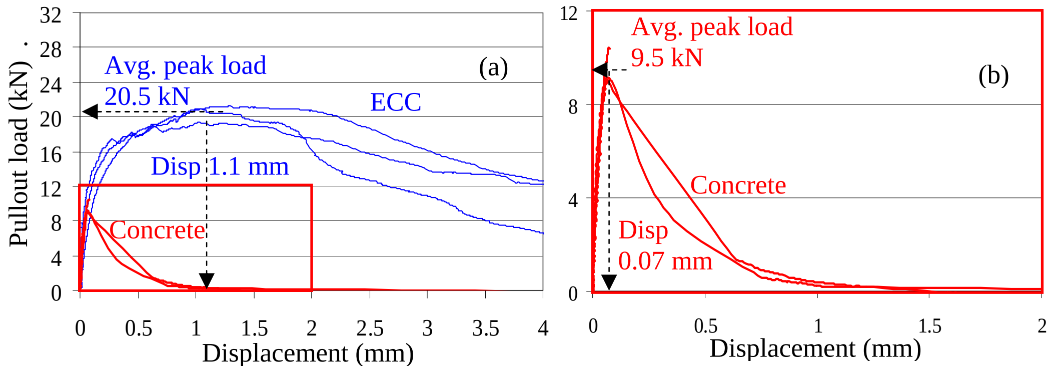

Figure 12: (a) Measured load as a function of displacement for pullout specimens for ECC and concrete, with the boxed area enlarged for clarity in (b).

Table 3 Material properties and structural behavior of concrete and ECC 2D pullout specimens

Material	ε_u (%)	f_c'(MPa)	F_N (kN)	F_M (kN)	S_c(mm)	w_c(μm)
Concrete 2	0.01*	45.6±1.0	10.0±0.1	9.5 ± 0.7	0.07 ± 0.01	~2000
ECC 2	2.5±0.4	41.7±0.5	9.6±0.0	20.5 ± 1.0	1.1 ± 0.2	57 ± 33

(ε_u: uniaxial tensile strain capacity; * assumed value; f_c': compressive strength; F_N: computed strength per anchor; F_M: measured strength per anchor; S_c: displacement (slip capacity); w_c: crack width; ±: standard deviation)

In Table 3, F_N is calculated utilizing Eqn (2) (adopted from analysis results of Ozbolt [16], the original equation is for specimen thickness equal to 100 mm, divided by 2 assuming it is valid for specimen thickness 50mm used in this investigation).

$$F_N = 28.5\sqrt{f_{cube}}\, d\,(1 + d/399.6)^{-1/2} \qquad (2)$$

with: f_{cube} = Concrete cube compressive strength (approximately equal to $1.22f_c'$ (MPa));
d = Embedment length of anchor (50mm in the present experiment);

Revealed in the Table 3, the measured strength F_M of the anchor/concrete connection is within 5% of the computed strength F_N. Conversely, the measured strength F_M of the anchor/ECC connection is about 20.5 kN, approximately 110% higher than the calculated values F_N. Again, this is mainly due to the fact that the compressive strength, a main contributing factor in the above equation for anchors in concrete, is not necessarily relevant to the failure of anchor/ECC connection, due to the switching of the failure mode from concrete fracture to ECC ductile damage process.

4.0 Conclusion

A new approach and material solution – exploiting ECC tensile ductility to suppress concrete material fracture failure in steel/concrete interaction zones was proposed and experimentally demonstrated through two sets of representative steel/ECC connection tests. Significant delay or elimination of fracture localization due to high stress concentration can be achieved via extensive inelastic straining offered by ECC, resulting in much improved structural performance in terms of load capacity and structural ductility. This material based solution to concrete fracture problems is expected to be applicable to broad classes of structural applications involving critical steel/concrete connections. Material ductility needs to be considered in design procedure for better prediction of structural performance of such critical connections made with ECC.

5.0 References:

1. Elfgren, L., *Round robin analysis and tests of anchor bolts in concrete structures*, Research report, RILEM TC 90-FMA, 1998.
2. Architectural Institute of Japan and Japan Society of Civil Engineers, *Records of the 1995 great Hanshin-Awaji earthauake disaster*, 1995, pp33.
3. Sheikh, T. M., Deierlein, G. G., "Beam-column moment connections for composite frames: Part 1," *Journal of structural engineering*, ASCE, 115(11), 1989, pp2858-2876.
4. Parra-Montesinos, G. and Wight, J. K., "Seismic response of exterior RC column-to-steel beam connetions," *Journal of structural engineering*, Oct., 2000, pp1113-1121.
5. Breen, J.E. et al, *Anchorage Zone Reinforcement for Post-Tensioned Concrete Girders*, National Cooperative Highway Research Program Report 356, Washington D.C.,1994, pp204.
6. Shama, A.A., Mander, J. B., and Aref, A. J, "Seismic performance and retrofit of steel pile to concrete cap connections," *ACI structural journal*, Jan, 2002, pp51-61.
7. Li, V.C., "From Micromechanics to Structural Engineering--the Design of Cementitous Composites for Civil Engineering Applications," *JSCE J. of Structural engineering and Earthquake Engineering*, Vol. 10, No.2, 1993, pp37-48.
8. Li, V.C. and Kanda,T., "Engineered Cementitious Composites for Structural Applications," Innovations Forum in ASCE, *J. Materials in Civil Engineering*, May 1998, pp66-69.
9. Li, V. C., Wang, S. and Wu, C. "Tensile Strain-hardening Behavior of PVA-ECC," *ACI Materials Journal*, Vol. 98, No. 6, Nov.-Dec., 2001, pp 483-492.
10. Li, V.C., Mishra, D.K., Naaman, A.E., Wight, J.K., Wu, H.C. and Inada, Y., "On the Shear Behavior of Engineering Cementitious Composites," *J. of Advanced Cement Based Materials*, Vol. 1, No. 3, March, 1994, pp142-149.
11. Kanda, T., Watanabe, W. and Li, V.C., "Application of Pseudo Strain hardening Cementitious Composites to Shear Resistant Structural Elements," Fracture Mechanics of Concrete Structures, *Proceedings of FRAMCOS-3*, AEDIFICATIO Publishers, Freiburg, Germany, 1998, pp1477-1490.
12. Kesner, K. E., and Billington, S. L., "Experimental Response of Precast Infill Panels made with DFRCC," *Proceedins of JCI Workshop on DFRCC*, Oct. 2002, pp289-298.
13. Fukuyama, H., Matsuzaki,Y., Nakano, K. and Sato, Y., "Structural Performance of Beam Elements with PVA-ECC," in *Proc. Of High Performance Fiber Reinforced Cement Composites 3 (HPFRCC 3)*, Ed. Reinhardt and A. Naaman, Chapman & Hull, 1999, pp531-542.
14. Ollgaard, J. G., Slutter, R. G. and Fisher, J.W., "Shear Strength of Stud Connectors in lightweight and Normal-Weight Concrete," *AISC Engineering Journal*, April, 1971, pp55-64.
15. AASHTO, *AASHTO LRFD bridge design specifications*, 2nd edition, American Association of State Highway and Transportation Officials, Washington D.C., 1998, 1052p.
16. Ozbolt, J., "Round-Robin Analysis of Anchor Bolts," *Research report – Round Robin Analyses and Tests of Anchor Bolts in Concrete Structure*, RILEM TC 90-FMA, Fracture Mechanics of Concrete – Applications, Edited by Lennart Elfgren, July 1998, pp15-1--28.